PAPER

NJC
www.rsc.org/njc

Spectroscopic characterization of an assembled pair of free-base and zinc porphyrins linked by the cyclic β-sheet peptide Gramicidin S†

Toru Arai,*[a] Koji Araki,[a] Naoki Maruo,[a] Yuko Sumida,[a] Chie Korosue,[a] Kengo Fukuma,[a] Tamaki Kato[b] and Norikazu Nishino*[b]

[a] *Faculty of Engineering, Kyushu Institute of Technology, Kitakyushu 804-8550, Japan. E-mail: arai@che.kyutech.ac.jp*

[b] *Graduate School of Life Science and Systems Engineering, Kyushu Institute of Technology, Kitakyushu 808-0196, Japan*

Received (in Montpellier, France) 18th February 2004, Accepted 14th April 2004
First published as an Advance Article on the web 21st July 2004

A pair of porphyrins was linked to the Orn side chains of Gramicidin S [cyclo(–D-Phe–Pro–Val–Orn–Leu–)$_2$] and its derivatives *via* the amide bonds; the assorted porphyrins were characterized by various spectroscopic methods. The high-field shifts of the porphyrin signals in the ^{1}H NMR spectrum and the exciton-coupled Cotton effects in the CD spectrum of cyclo[–D-Phe–Pro–Val–Orn(Por)–Leu–]$_2$ are both intense compared to those of cyclo[–D-Phe–Pro–Val–Dab(Por)–Leu–]$_2$ or cyclo[–D-Phe–Pro–Val–Lys(Por)–Leu–]$_2$ (Dab, diaminobutyric acid; Por, the side-chain linked porphyrin). Some ^{1}H NMR signals of the tolyl protons of the porphyrins coalesce at 353 K in CD_2Cl_2, which reveals dynamic processes of the porphyrins. The intensities of the Cotton effect are: Gramicidin S with a pair of free-base porphyrins ≈ Gramicidin S with a free-base porphyrin and a zinc porphyrin < Gramicidin S with a pair of zinc porphyrins. The ^{1}H NMR, UV-vis, CD and fluorescence spectra show that the solvent substantially influences the assembly of the porphyrins. These spectroscopic studies suggest that the strength of the intramolecular interactions between a pair of porphyrins is in the order of toluene > CH_2Cl_2 > DMF.

Introduction

Various functional biomolecules such as hemes, chlorophylls and vitamin B_{12} contain porphyrins and related compounds as the active centers.[1] The rational arrangements of the tetrapyrroles, cofactors and so on in biosystems are essential for their excellent functions, for instance, charge separation,[2] solar energy collection[3] and redox catalysis.[4] Among various biomolecules, the planar structure of porphyrins with a hydrophobic conjugated system is unusual. A number of model systems has been constructed with oligomeric,[5] polymeric[6] and supramolecular porphyrins.[7] In particular, various porphyrin arrays linked by artificial polypeptides have been synthesized[8,9] by virtue of the recent progress in peptide synthesis.[10] The importance of peptide-linked porphyrins is increasing because natural proteins are not only the scaffolds of the porphyrins but also regulate the reactivities of the porphyrins.[11] The environments of the natural porphyrins such as neighboring amino acids, water molecules and lipophilic molecules substantially effect the function and assembling of porphyrins. The interactions between porphyrins are largely hydrophobic and π-π interactions,[12] in addition to hydrogen bonding and metal coordination;[2,3] therefore, the solvent may influence the relative orientation between porphyrins, that is, the orientation of the porphyrins could be tunable by the solvent.

Here we wish to introduce a new methodology to investigate the solvent effect for the interaction between porphyrins. A pair of porphyrins was linked to the antiparallel β-sheet strands of a cyclic decapeptide, Gramicidin S (GS). GS [cyclo(–D-Phe–Pro–Val–Orn–Leu–)$_2$, **2c**, Scheme 1][13] is a natural bacterial polypeptide comprised of a set of antiparallel β-sheets and two type II' β-turn units.[14] The cyclic framework of this small polypeptide stabilizes its β-sheet structure. The side chains of the Orn residues are in a face-to-face orientation, which can tether two functional molecules. A pair of porphyrins linked to the antiparallel β-sheet may take a face-to-face orientation, which will be characterized by spectroscopic methods. Short linkers such as –$(CH_2)_3$– between the porphyrin and peptide will avoid distortion of the peptide framework upon varying the solvent. Thus, a new tool to examine the solvent effect on the porphyrin assembly is designed using a spatially close pair of porphyrins on an antiparallel peptide template. We have briefly communicated the synthesis and the spectroscopic feature of the porphyrins linked to GS.[15] Here we report further investigations on the relative orientation of the porphyrins and its solvent dependency as characterized by various spectroscopic methods including ^{1}H NMR.

Results and discussion

Syntheses of Gramicidin S derivatives bearing a pair of porphyrins and the ^{1}H NMR investigation of the peptide conformation

A GS derivative bearing a pair of porphyrins at the Orn side chains, cyclo[–D-Phe–Pro–Val–Orn(PorFb)–Leu–]$_2$ [**2d**, PorFb is 4-(10,15,20-tritolylporphyrin-5-yl)benzoyl], and its two homologs with different spacer lengths between the peptide and porphyrins, cyclo[–D-Phe–Pro–Val–Dab(PorFb)–Leu–]$_2$ (**1d**) and cyclo[–D-Phe–Pro–Val–Lys(PorFb)–Leu–]$_2$ (**3d**), were prepared (Scheme 1). First, the GS derivatives and homologs

† Electronic supplementary information (ESI) available: complete synthetic details and characterization of the GS derivatives. See http://www.rsc.org/suppdata/nj/b4/b402541e/

DOI: 10.1039/b402541e

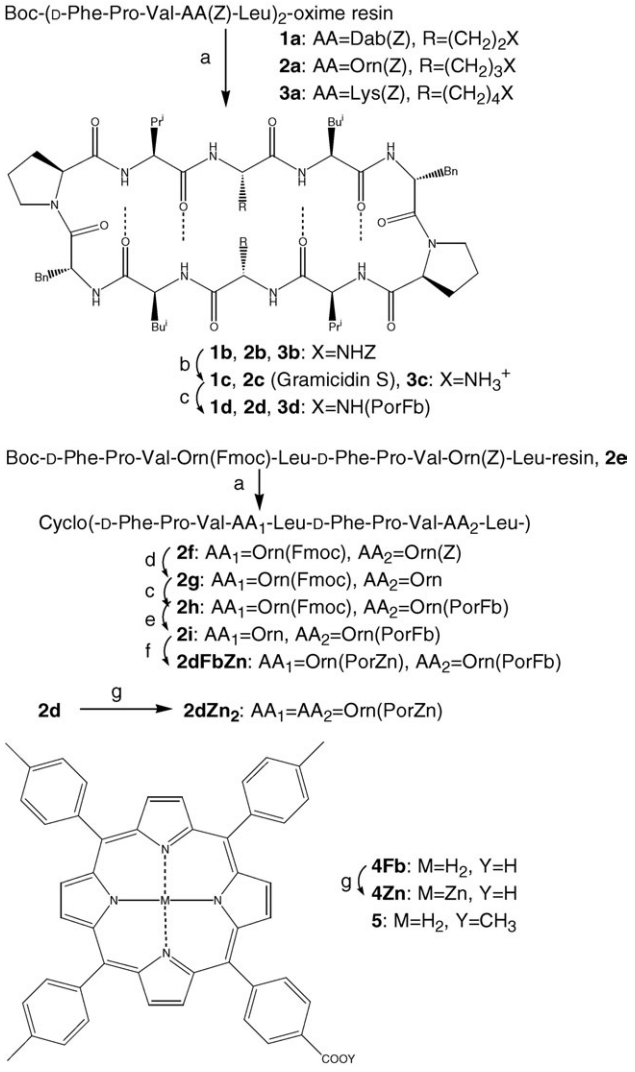

Scheme 1 Synthesis of Gramicidin S derivatives bearing a pair of porphyrins. (a) TFA, then AcOH/*N*,*N*-diisopropylethyamine; (b) H_2; (c) **4Fb**, PyBOP, HOBt; (d) TFA/thioanisole/*m*-cresol; (e) piperidine; (f) **4Zn**, PyBOP, HOBt; (g) $Zn(OAc)_2$.

with the Z protections on the side chains (**1a**–**3a**) were synthesized *via* a cyclization-cleavage method from the decapeptide-linked oxime resin (*p*-nitrobenzophenone oxime resin).[14c,16] That is, after the removal of the N-terminal Boc group of the Boc–[D-Phe–Pro–Val–AA(Z)–Leu]$_2$–oxime resin (**1a**, AA = Dab; **2a**, Orn; **3a**, Lys), the resin was treated with AcOH/*N*,*N*-diisopropylethylamine (2 molar equiv each) for 2 h to yield cyclo[–D-Phe–Pro–Val–AA(Z)–Leu–]$_2$ (**1b**,[17] AA = Dab; **2b**,[17,18] Orn; **3b**,[14d,17] Lys) in 70, 84 and 91% yields, respectively. The Z groups were then removed and 4-(10,15,20-tritolylporphyrin-5-yl)benzoic acid (**4Fb**)[5b] was condensed onto each side chain NH_2 group to yield **1d**, **2d** and **3d** in 74, 86 and 81% yields, respectively.

The GS derivative bearing one Zn porphyrin (PorZn) and a free-base porphyrin (PorFb) was synthesized from the cyclic decapeptide with two different protective groups, cyclo[–D-Phe–Pro–Val–Orn(Fmoc)–Leu–D-Phe–Pro–Val–Orn(Z)–Leu–] (**2f**), which was prepared from **2e** by the cyclization-cleavage method. The Z protection was selectively removed by TFA/thioanisole/*m*-cresol[19] to yield **2g**, to which **4Fb** was condensed to yield **2h** bearing one Orn(Fmoc) and an Orn(PorFb). The Fmoc group of **2h** was removed by piperidine to yield **2i**, and then **4Zn** was condensed to yield **2dFbZn** bearing one Orn (PorZn) and one Orn(PorFb). This method may be applicable to the synthesis of other GS derivatives bearing different functional groups. The metallation of **2d** with excess $Zn(OAc)_2$ afforded **2dZn$_2$** bearing a pair of Orn(PorZn) residues. The UV-vis spectrum of **2dFbZn** was almost the average of those of **2d** and **2dZn$_2$** in CH_2Cl_2 (Fig. 1), suggesting that there was little ground-state interaction between the porphyrins[5c] in this solvent (see below). The HPLC confirmed the purity of all the GS derivatives and ^{1}H NMR (1D and 2D COSY) and FAB MS/FAB HR-MS spectra characterized their structures.

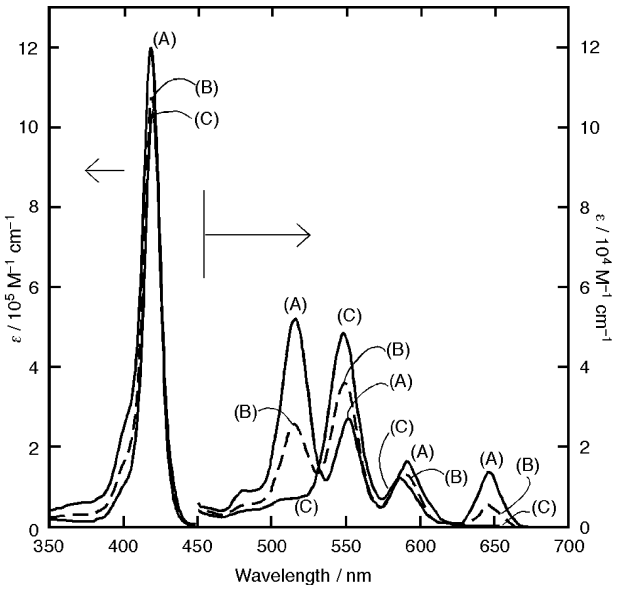

Fig. 1 UV-vis spectra of **2d** (trace A), **2dFbZn** (trace B, broken line) and **2dZn$_2$** (trace C) in CH_2Cl_2.

^{1}H NMR measurements of the GS derivatives bearing a pair of porphyrins in DMSO-d_6 (0.80 mM) show that their cyclic frameworks take on a conformation similar to that of the natural GS (**2c**) in this solvent (Table 1). The temperature dependencies of the Val–NH ($\Delta\delta = -2.0$ ppb K^{-1}, ppb = ppm × 10^{-3}) and Leu–NH (−2.6 ppb K^{-1}) signals of **2d** are as small as those of **2c**.[14c] These facts support the intramolecular hydrogen bonds Val–NH···OC–Leu and Leu–NH···OC–Val, as shown in the crystal structure of **2c**.[14a] The large temperature dependencies of the Orn–αNH and D-Phe–NH signals of both **2c** and **2d** show that these NHs are not involved in intramolecular hydrogen bonding and are exposed to the solvent DMSO.[20] The coupling constants of Val–NH, Orn–αNH and Leu–NH of both **2c** and **2d** ($^3J_{NH\alpha}$ = 8.6–10.4 Hz) show that these residues are involved in the β-sheet structure, while the D-Phe residues (J = 2.7–3.7 Hz) are involved in the β-turn.[21] In fact, the NOESY spectra of **2d** show cross peaks between Val–CαH and Orn–NH, between Orn–CαH and Leu–NH, between Leu–CαH and D-Phe–NH, but not between Pro–CαH and Val–NH. These NOESY peaks support the hypothesis that the –Val–Orn–Leu–D-Phe–

Table 1 ^{1}H NMR chemical shifts, coupling constants and temperature coefficients of the amide protons of GS derivatives in DMSO-d_6[a]

	δ/ppm ($^3J_{HN\alpha}$/Hz) $\Delta\delta$/ppb K^{-1}			
	2c (GS)[b]	**2d**	**2dZn$_2$**	**3d**
Val–NH	7.20 (9.5)	7.30 (10.4)	7.33 (9.5)	7.29(9.5)
	−1.8	−2.0	−2.1	−2.1
Orn–αNH	8.65 (9.5)	8.66(9.8)	8.73 (9.5)	8.59 (9.5)
	−4.8	−4.5	−4.5	−5.3
Leu–NH	8.31 (9.2)	8.50 (8.6)	8.53 (8.5)	8.46 (8.9)
	−2.7	−2.6	−2.8	−2.1
D-Phe–NH	9.04 (3.7)	8.93 (2.7)	8.99 (2.5)	8.91 (3.7)
	−7.0	−8.3	−7.4	−8.6

[a] δ and $^3J_{HN\alpha}$ were measured at 303 K, while $\Delta\delta$ is at 303, 313, 323 and 333 K. [b] Ref 14*c*. [c] At 313 K.

sequence in **2d** constructs a β-sheet structure[22] similar to that of **2c**. The ^{1}H NMR measurements of the other GS derivatives bearing porphyrins, **1d**, **3d**, **2dFbZn** and **2dZn$_2$**, show essentially the same results. The derivation of GS at the Orn (or Dab/Lys) side chain did not distort the conformation of the peptide framework comprised of a set of antiparallel β-sheets and β-turns. ^{1}H NMR spectra in DMSO-d_6 and D_2O–H_2O have already been employed to examine the relationship between peptide conformation and the NMR data (δ, $\Delta\delta$ and J).[20–22] Therefore, we do not discuss the peptide conformation of these GS derivatives in a solvent other than DMSO, such as in toluene or dichloromethane (GS derivatives are insoluble in water).

^{1}H NMR investigation of the assembled porphyrins and the solvent effect

The ^{1}H NMR spectra of **2d** also show a spatially close pair of porphyrins on the cyclic polypeptide. In DMF-d_7, the reference monomeric porphyrin, 5-*p*-methoxycarbonylphenyl-10,15,20-tritolylporphyrin (**5**), has a simple ^{1}H NMR spectrum (data not shown). The pyrrole-β protons of **5** appear at δ 8.95 (s, 8H) and three tolyl groups appear at δ 8.20 (d, 6H), 7.70 (d, 6H) and 2.72 (s, 9H). That is, the tolyl groups cis to the methoxycarbonylphenyl group and the trans tolyl group appear at the same chemical shifts. In contrast, the ^{1}H NMR spectrum of **2d** in DMF-d_7 (2.0 mM, 500 MHz) is more complex. The pyrrole-β protons of **2d** appear at δ 8.89 (m, 12H) and 8.76 (d, 4H, overlapped with an NH signal) at 303 K [Fig. 2(a), for the discussion of the pyrrole-β signals, see below]. The tolyl signals of **2d** appear as three sets, namely tolyl-A [δ 8.18 (d, 4H), 7.69 (d, 4H) and 2.71 (s, 6H)], tolyl-B (δ 8.01, 7.45 and 2.52) and tolyl-C (δ 7.98, 7.38 and 2.52). The aromatic signals of tolyl-B and C overlap with each other and also with the solvent signal (DMF), Val–NH and the side chain of Phe. However, a careful inspection of the spectrum, including the signal intensity, measurement at elevated temperature (see below) and the 2D^{1}H–^{1}H COSY spectrum [Fig. 2(b)] unambiguously indicated the existence of three magnetically non-equivalent tolyl groups for **2d**. In the 2D COSY spectrum, three cross peaks appear between the tolyl ortho (to porphyrin) and meta protons. Moreover, long-range COSY signals (not shown) appear between the tolyl meta protons and tolyl-Me protons, that is, between the signals at δ 8.18 and 2.71, between δ 7.45 and 2.52 and between δ 7.38 and 2.52. Thus, the three tolyl groups of a porphyrin in **2d** are non-equivalent at 303 K, which attests to the unsymmetrical character of the porphyrins. Fig. 2(d) depicts a speculative molecular profile of **2d** in DMF, having an edge-to-edge orientation of the porphyrins with an offset. The chemical shifts of tolyl-A of **2d** are similar to those of the tolyl groups of **5**, which means that these protons are not affected by the ring current of the other porphyrin. The tolyl-B and C are high-field shifted compared to tolyl-A, probably affected by the ring current of the other porphyrin existing nearby.‡ At 353 K, the pyrrole-β protons of **2d** appear as four doublet peaks at δ 8.87 (4H), 8.84 (4H), 8.82 (4H) and 8.72 (4H) [Fig. 2(c)]. Tolyl-A is shifted slightly (δ 8.14, 7.66 and 2.71); however, tolyl-B and C show coalescence phenomena at this temperature, with their signals at δ 7.94, 7.42 and 2.53. These facts suggest a dynamic process within the time scale of NMR.[23] The coalescence of tolyl-B and C suggests a symmetrical character of the porphyrin at 353 K. The appearance of four doublet signals for the pyrrole-β protons supports the symmetrical character of the porphyrin. This interpretation may account for the complex signals appearing for the pyrrole-β protons at 303 K [Fig. 2(a)]. The coalescence at 353 K

‡ The reason why the signals of tolyl-B are high-field shifted is not yet clear. However, the dynamic exchange between tolyl-B and C described below may account for this.

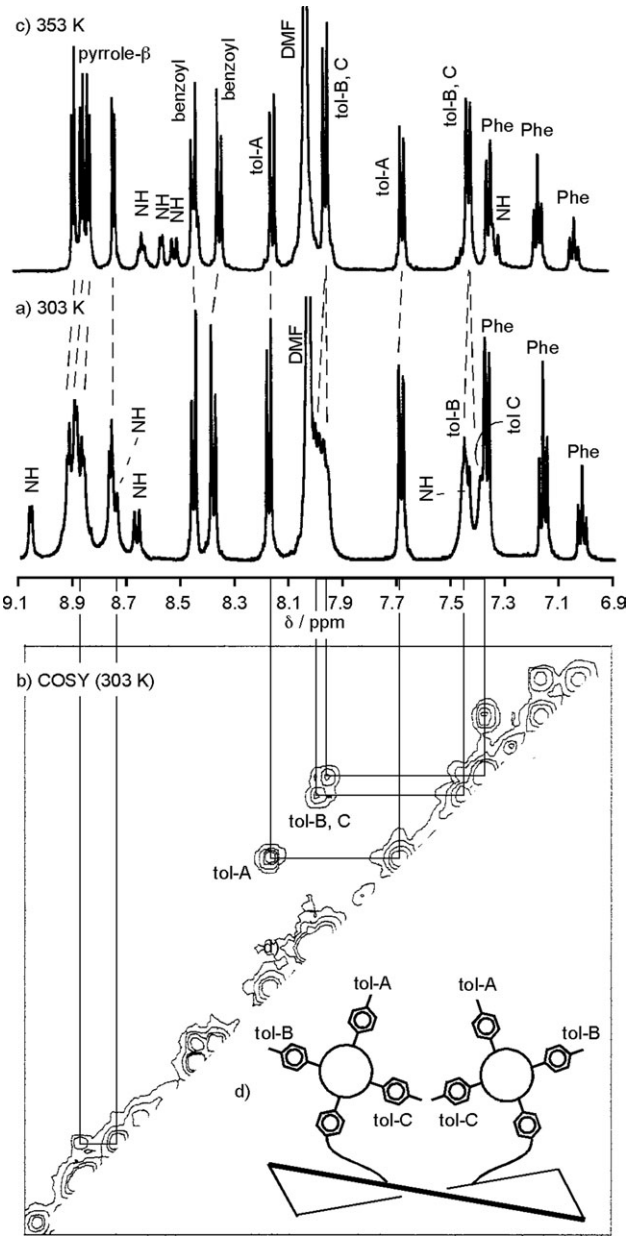

Fig. 2 ^{1}H NMR spectra (in DMF-d_7, aromatic region) of **2d**: (a) 1D, (b) 2D COSY at 303 K; (c) 1D at 353 K and (d) an illustration depicting three non-equivalent tolyl groups.

suggests that the spacer between the porphyrin and peptide is slightly flexible or that the rotation of the porphyrin ring along the porphyrin–Orn side-chain axis is slightly restricted; however, further examination in this solvent failed because of the poor peak separation for tolyl-B and C.

In CD_2Cl_2 (2.0 mM), the ^{1}H NMR signals of **2d** are broadened compared to those in DMF-d_7. The pyrrole-β protons of **2d** (2.0 mM) appear as four doublet peaks, for instance at 303 K, at δ 8.75, 8.61, 8.56 and 8.33 [Fig. 3(a)]. Their couplings with each other were confirmed by the 2D COSY spectra [Fig. 3(b)] and the obstructive NH signals could be eliminated when the solution of **2d** was treated with CD_3OD (data not shown). In CD_2Cl_2, the three magnetically non-equivalent tolyl signals are fairly well separated from each other. The signals of tolyl-A at δ 8.02 and 7.53 [at 303 K, Fig. 3(a)] are sharp and their chemical shifts are close to those of the tolyl groups of **5** (δ 8.10 and 7.59 in CD_2Cl_2). The signals of tolyl-B (δ 7.46 and 6.91) and tolyl-C (δ 7.29 and 6.73) are significantly broadened at 303 K, which suggests the involvement of some dynamic process. These well-separated signals of tolyl-B and C [compare the COSY cross peaks of Figs. 2(b) and

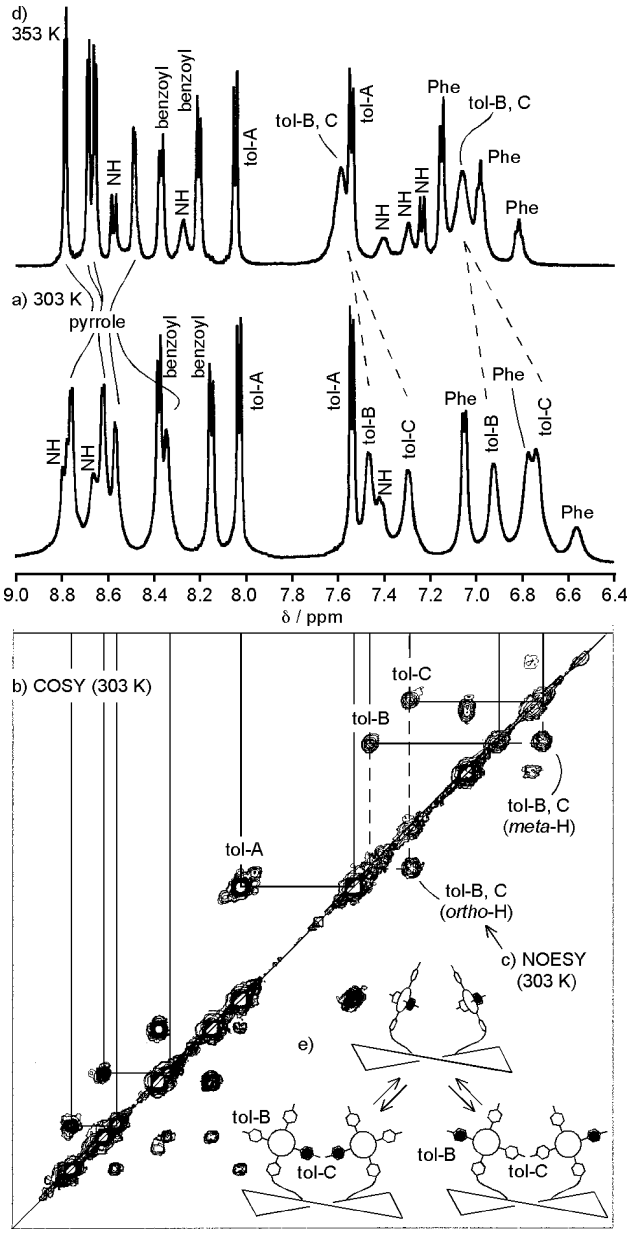

Fig. 3 ^{1}H NMR spectra (in CD_2Cl_2, aromatic region) of **2d**: (a) 1D, (b) 2D COSY, (c) 2D NOESY at 303 K; (d) 1D at 353 K and (e) an illustration depicting the dynamic behavior of a pair of porphyrins.

3(b)] help further investigations on the dynamic processes. (1) The dynamic process including the tolyl-B and C groups is observed in the 2D NOESY spectra [Fig. 3(c)]. It is known that the proton signals involved in the chemical exchange process often show pseudo-NOESY cross peaks.[23b] Fig. 2(c) clearly shows the cross peaks between tolyl-B (ortho) and tolyl-C (ortho) and between tolyl-B (meta) and tolyl-C (meta) protons. (2) The CD_2Cl_2 solution of **5b** was heated in an NMR sample tube fitted with a pressure/vacuum valve to observe the coalescence of the peaks of tolyl-B and C at 353 K [Fig. 3(d)] At this temperature, the signals of pyrrole are sharpened compared to those at 303 K; however, the signals of tolyl-B and C are still broadened. (3) Finally, the spin-saturation transfer technique was applied to the chemical exchange process of tolyl-B and C.[23c] Irradiating the tolyl-C signal (ortho, δ 7.29) at 303 K caused spin-saturation transfer to the signal of tolyl-B (ortho, δ 7.46), and the intensity of the latter signal became 33% of the intensity before the saturation of tolyl-C (data not shown). From the equation[23c]

$$k = (M_{0B}/M_B - 1)/T_{1B}$$

the rate constant k for the chemical exchange process including the tolyl-B and C was estimated to be 0.92 s^{-1}. M_{0B} and M_B are the signal intensities of signal B before and after the spin-saturation, T_{1B} is the spin-lattice relaxation time for signal B (2.22 s in this case). Fig. 3(e) depicts a hypothetical illustration of the dynamic process involved in **2d**. In this figure, the rotation of the porphyrin along the porphyrin–Orn side-chain axis interchanges the tolyl C and tolyl B groups. Three tolyl groups of a porphyrin are non-equivalent at 303 K and some signals coalescence at the elevated temperature. The sharp four doublet signals of pyrrole-β protons at 353 K suggest the symmetrical character of the porphyrin.

It is interesting that the tolyl-B and C signals are still broadened at 353 K but that the pyrrole-β signals are sharp at that temperature [Fig. 3(d)]. As one of the reviewers pointed out, four AB systems (eight doublets) are expected for the pyrrole-β signals of the slow exchange system of **2d**. In fact, sharp four doublets appear in DMF-d_7, CD_2Cl_2 and toluene-d_8 (described below) at 353 K and broadened signals or complex multiplet signals appear at 303 K. Low-temperature ^{1}H NMR measurements (303 to 208 K, 2.0 to 0.5 mM) were tried in CD_2Cl_2, in the expectation of spectral changes; however, the signals were broadened without any change of chemical shifts, intensity and couplings for the porphyrin signals. Probably intermolecular aggregation occurs at low temperature (polypeptides are hardly soluble in dichloromethane).

In toluene-d_8 (2.0 mM), the ^{1}H NMR signals of **2d** are extremely broadened at 303 K [Fig. 4(a)] and, as a matter of fact, no information could be obtained from this spectrum. In this solvent, **2d** shows sharpened ^{1}H NMR signals at 353 K [Fig. 4(b)] in which the spectral profile resembles that in CD_2Cl_2 at 353 K [Fig. 3(d)], with four sets of pyrrole protons and two sets of tolyl signals. The extremely broadened signals of **2d** at 303 K are probably due to aggregation of the porphyrins in toluene-d_8. No obvious spectrum change was observed when the concentration of **2d** was varied from 1.0 to 4.0 mM at 303 K. However, no direct and clear evidence has been obtained yet on whether the porphyrins assemble in toluene intramolecularly or intermolecularly.

In any case, these ^{1}H NMR spectra of **2d** show that in DMF-d_7, CD_2Cl_2 and toluene-d_8 some of the tolyl groups are affected by the ring current of another porphyrin, which means that the porphyrins are located close to each other on the polypeptide

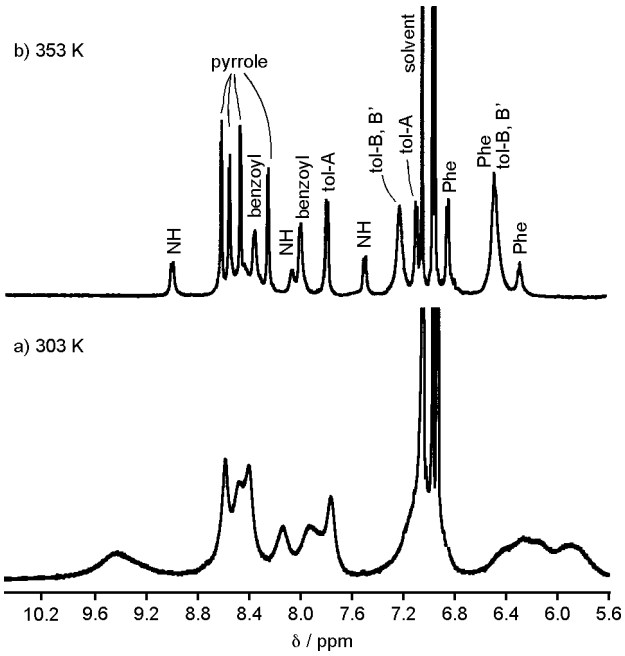

Fig. 4 ^{1}H NMR spectra (in toluene-d_8, aromatic region) of **2d**: at (a) 303 K and (b) 353 K.

template. The magnetic non-equivalence between tolyl-B and C suggests that the porphyrins are unsymmetrically arranged. That is, the porphyrins are not in a symmetric face-to-face orientation but probably in a side-by-side orientation with an offset as depicted in Figs. 2(d) and 3(e), although the detailed structure of **2d** is not yet clear because no single crystal has been obtained (for UV-vis and CD spectral results, see below). Comparing the ^{1}H NMR spectra of **2d** in DMF-d_7, CD_2Cl_2 and toluene-d_8 (Figs. 2–4), the signal width becomes broader in the order DMF-d_7 < CD_2Cl_2 < toluene-d_8 (at both 303 and 353 K). This order may reflect the kinetics of the chemical exchange process involved in **2d** or the stability of the aggregated porphyrins in the solvent examined.

It is interesting that the high-field shift of the tolyl groups of the porphyrins is in the order of **1d** < **3d** < **2d**; for instance, the high-field-shifted tolyl protons (meta to porphyrin) of **1d**, **2d** and **3d** appear at 7.35, 7.23 and 7.33 ppm (in DMSO-d_6), respectively. These facts might mean that the porphyrins in **2d** are assembled more closely than those in **1d** and **3d**, which is an unexpected result because the spacer length between the porphyrin and peptide follows the order: **1d** < **2d** < **3d**. This result is concerned with the CD results of these GS derivatives described below.

It may be noted here that the chemical shifts of PorFb and PorZn were too close to distinguish; therefore, the NOESY experiment of **2dFbZn** to examine the orientations of PorFb and PorZn failed.

CD investigation on the orientation of porphyrins bound to the GS framework

The GS derivatives bearing a pair of PorFb, **1d**, **2d** and **3d**, show similar UV-vis spectra in CH_2Cl_2, with λ_{max} at around 420, 516, 552, 592 and 646 nm (see Fig. 1). In the same solvent, **1d**, **2d** and **3d** show different CD spectra [Fig. 5(a)]. Split Cotton effects appear for **1d** in the porphyrin Soret band region at 421 nm [Fig. 5(a), trace A, $\Delta\varepsilon = -25.9$ M^{-1} cm^{-1}] and 414 nm ($\Delta\varepsilon = 11.1$ M^{-1} cm^{-1}), which are slightly unsymmetrical. Split Cotton effects also appear for **2d** at 424 nm [Fig. 5(a), line B, $\Delta\varepsilon = -52.9$ M^{-1} cm^{-1}] and 416 nm ($\Delta\varepsilon = 27.9$ M^{-1} cm^{-1}), in which the mid-point of two symmetric CD bands (420 nm) corresponds to the UV absorption. These split Cotton effects are assigned to the exciton-coupled CD that arises from two porphyrin chromophores. It is known that the two porphyrin rings located near each other in the chiral orientation show exciton-coupled Cotton effects in the porphyrin Soret band region, which are characterized by two symmetrically split intense bands with inverse signs.[24] The pair of porphyrins of **2d** located near each other on the cyclic peptide and their chiral orientations are determined by the peptide framework. In contrast, **3d** shows a weak single CD band at 420 nm ($\Delta\varepsilon = -17.0$ M^{-1} cm^{-1}), which is assigned to the CD induced by the chiral amino acids or the side-chain phenyl groups of the D-Phe residue,[25] not the exciton-coupled CD. The longer –$(CH_2)_4$– spacers between the porphyrin and peptide in **3d** would account for its weak CD, although the reason why **2d** shows an intense CD compared to **1d** is yet unclear. It is interesting that the high-field shifts of the tolyl proton signals in ^{1}H NMR are in the order of **1d** < **3d** < **2d** as described above, which may be associated with the order of the CD intensities of **3d** < **1d** < **2d**. It should be noted here that the CD spectra were taken at 1.6 μM peptide concentration, in which the peptide concentrations were determined by the amino acid analysis (see Experimental). However, no concentration dependency was observed in the 0.4 to 16 μM concentration range.

Next, the effect of Zn metallation of the porphyrin on the exciton-coupled CD was examined using **2d**, **2dFbZn** and **2dZn$_2$**. In CH_2Cl_2, **2dFbZn** shows a CD spectrum similar to that of **2d** [Fig. 5(b)]. The similar CD and the absorption

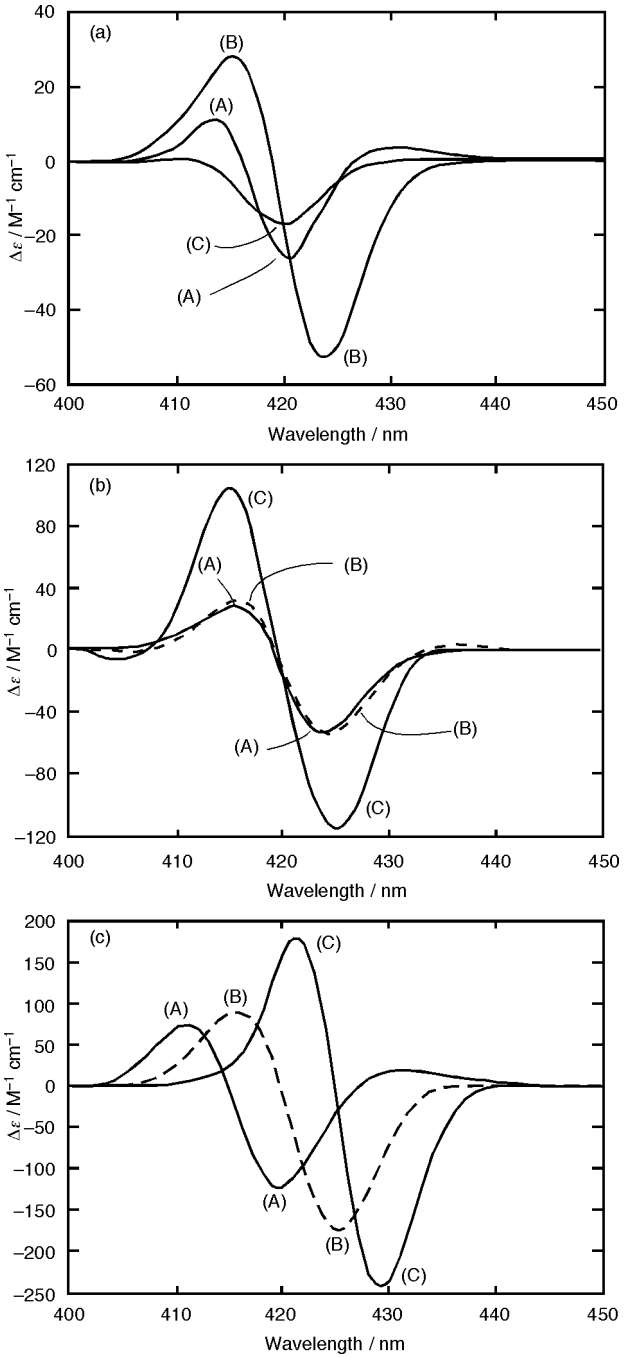

Fig. 5 CD spectra of (a) **1d** (trace A), **2d** (trace B) and **3d** (trace C) in CH_2Cl_2; (b) **2d** (trace A), **2dFbZn** (trace B, broken line) and **2dZn2** (trace C) in CH_2Cl_2 and (c) **2d** (trace A), **2dFbZn** (trace B, broken line) and **2dZn$_2$** (trace C) in MeOH ([peptide] = 1.6 μM).

spectra in the Soret band region of **2dFbZn** and **2d** suggest that Zn porphyrin and the free-base porphyrin behave similarly in the CD event. In contrast, intense Cotton effects appear for **2dZn$_2$**at 425 nm ($\Delta\varepsilon = -114.2$ M^{-1} cm^{-1}) and at 415 nm ($\Delta\varepsilon = 101.3$ M^{-1} cm^{-1}). Zn porphyrins are usually of low solubility compared to the free-base porphyrins, which possibly accounts for the intramolecular assembling of PorZn in **2dZn$_2$** to show the intense Cotton effects. The same tendency for Cotton effects was observed in MeOH [Fig. 5(c)]; **2d** and **2dFbZn** show similar CD spectra except for their wavelength. The different wavelengths of the Cotton effects reflect the different UV absorptions, λ_{max} in MeOH is 415 nm for **2d**, 420 nm for **2dZn$_2$** and two λ_{max} (416 and 421 nm) are found for **2dFbZn**. Again, **2dZn$_2$** shows an intense CD compared to **2d** and **2dFbZn** in MeOH. The Cotton effects of these three compounds in MeOH are more intense than those in CH_2Cl_2 (for the solvent effect on the CD spectra, see below).

Further solvent effects for the intramolecular assembling of two PorZn in **2dZn$_2$** were examined in toluene, triethyl phosphate, TFE, pyridine and DMF (Table 2), besides CH_2Cl_2 and MeOH described above. The Cotton effects are solvent-dependent, varying in their intensities, wavelengths and profiles. As for the intensities of the Cotton effects of **2dZn$_2$**, strong Cotton effects appeared in toluene at 435 nm ($\Delta\varepsilon = -288.3$ M^{-1} cm^{-1}), 427 nm ($\Delta\varepsilon = 386.3$ M^{-1} cm^{-1}) and 418 nm ($\Delta\varepsilon = -70.8$ M^{-1} cm^{-1}). It is not yet clear why **2dZn$_2$** shows such an unsymmetrical CD spectra in toluene.[24g] The CD spectra of **2dZn$_2$** in the other solvents are all weaker than that in toluene and the order of intensities, A, is: toluene > MeOH > triethyl phosphate > TFE > CH_2Cl_2 > pyridine > DMF. This order is not associated with the dielectric constant, dipole moment or the acceptor/donor character of the solvents.[26] The coordination of the solvent to Zn or the solubility of porphyrins is not related to this observed order of the solvent effect. However, the order of the Cotton effect intensity is in line with the π* scale, which is an index of solvent dipolarity/polarizability and reflects the ability of the solvent to stabilize a charge or a dipole.[26,27] The reported values of the π* parameter are 0.54 (toluene), 0.60 (MeOH), 0.72 (triethyl phosphate), 0.73 (TFE), 0.82 (CH_2Cl_2), 0.87 (pyridine) and 0.88 (DMF).[27b] In a solvent with a lesser ability to stabilize a dipole, such as toluene with a small π* parameter, the porphyrins may prefer the assembled structure. This interpretation agrees with the electrostatic model for porphyrin-porphyrin stacking in non-aqueous media.[12]

The Cotton effects of **2dZn$_2$** appear at different wavelengths depending on the solvents but essentially appear around the λ_{max} of the absorption spectra. The λ_{max} value of **2dZn$_2$** differs in various solvents but is the same as the λ_{max} value of Zn tetramesitylporphyrin (ZnTMP) in the same solvent, except in toluene. In toluene only, the λ_{max} of **2dZn$_2$** (424 nm) is red-shifted and shows a shoulder peak at around 435 nm (trace B in Fig. 6), in contrast to the sharp peak of ZnTMP at 421 nm (data not shown). In the other solvents examined, for instance in CH_2Cl_2 (trace A in Fig. 6), the Soret absorption of **2dZn$_2$** is not red-shifted compared to ZnTMP and no shoulder peak is observed. This fact supports the interpretation that the two porphyrins in **2dZn$_2$** favor an associated structure in toluene, probably in the side-by-side fashion. Based on Kasha's theory about exciton coupling and the orientation of the transition moment in porphyrins, the long-wave shift in the absorption spectra arises from the side-by-side interaction of the chromophores,[28] which is often observed in water-soluble porphyrins[29] and dimeric porphyrins linked in a side-by-side fashion.[5f]

In order to support the side-by-side orientation of the pair of porphyrins in **2dZn$_2$**, 4,4′-dipyridyl was added to intramolecularly bridge the zinc porphyrins.[30] When the solution of **2dZn$_2$** in CH_2Cl_2 (20 μM) was titrated with 4,4′-dipyridyl, the absorption of **2dZn$_2$** at 421, 550 and 589 nm shifted to 426, 562 and 603 nm with clear isosbestic points [Fig. 7(a)].[15b] Interestingly, the exciton-coupled Cotton effect of **2dZn$_2$** [Fig. 5(b), trace C]

Table 2 The exciton-coupled Cotton effects in the CD spectra of **2dZn$_2$**[a]

Solvent	λ_{ext}/nm ($\Delta\varepsilon$/M^{-1} cm^{-1})			A
Toluene	435 (−288.3)	427 (386.3)	418 (−70.8)	−675
MeOH	425 (−243.5)	415 (180.2)		−424
Triethyl phosphate	429 (−175.8)	421 (124.7)		−301
TFE	423 (−152.8)	414 (106.6)		−259
CH_2Cl_2	425 (−114.2)	415 (101.3)		−216
Pyridine	434 (−133.8)	428 (67.1)		−201
DMF	432 (−115.0)	424 (60.7)		−176

[a] 1.6 μM at 298 K. λ_{ext}, peak of trough wavelength; A, couplet amplitude.

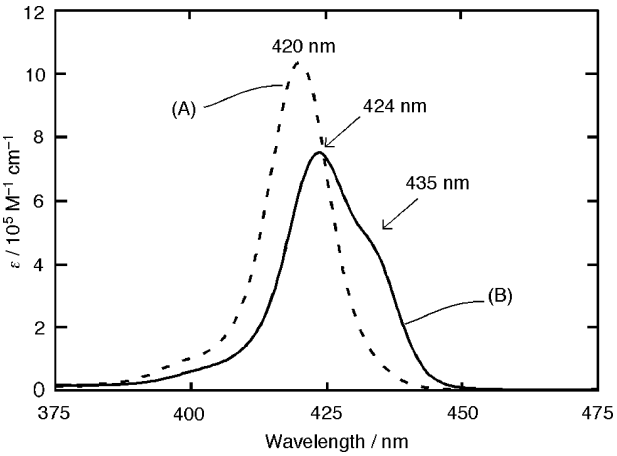

Fig. 6 UV-vis spectra of **2dZn$_2$** in CH_2Cl_2 (trace A) showing the sharp Soret band and in toluene (trace B) showing a shoulder peak (1.0 μM).

disappears upon the addition of 4,4′-dipyridyl, to show a weak induced CD at 424 nm [$\Delta\varepsilon = 23.7$ M^{-1} cm^{-1}, Fig. 7(b)]. A hypothetical interpretation of this result is that the pair of porphyrins in **2dZn$_2$** takes a side-by-side orientation without 4,4′-dipyridyl as described above and the chiral orientation between the porphyrins is determined by the peptide framework (see below). However, when an excess of 4,4′-dipyridyl is added, this diamine ligand forms a host-guest complex with **2dZn$_2$**. The intramolecular bridging by 4,4′-dipyridyl may bring the pair of porphyrins to a face-to-face orientation [Fig. 7(c), right]; therefore, merely a weak Cotton effect appears for the mixture of **2dZn$_2$** and 4,4′-dipyridyl. Thus, the addition of 4,4′-dipyridyl might change the side-by-side orientation of porphyrins in **2dZn$_2$**.

The exciton-coupled Cotton effects of **2d**, **2dFbZn** and **2dZn$_2$** in all the solvents examined have (−+) sign [from longer to shorter wavelengths; see Figs. 5(b), 5(c)], although the Cotton effect is sometimes distorted. From the exciton chirality method, the (−+) sign of the Cotton effect means a negative chirality, which arises from two excitons in a left-twisted arrangement.[24c] Because the β-strands of the natural polypeptide including GS are generally left-twisted,[31] the exciton

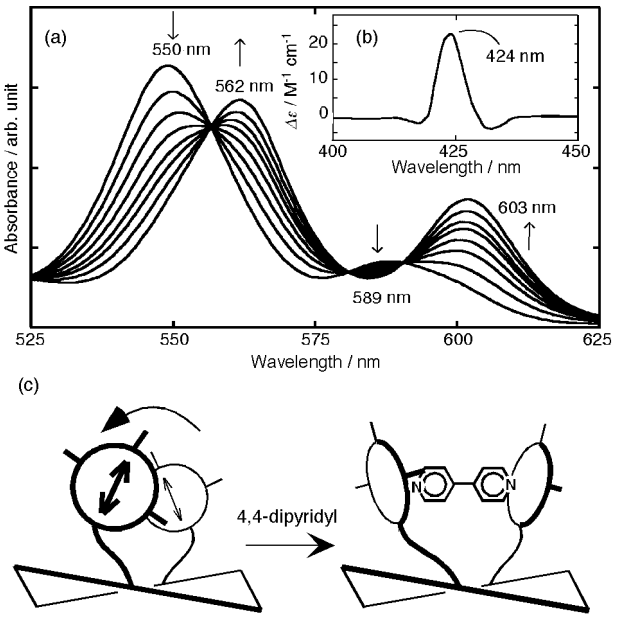

Fig. 7 (a) UV-vis spectra of the titration of **2d** (20 μM in CH_2Cl_2) by 4,4′-dipyridyl (0, 0.2, 0.4. . .2.0 equiv). (b) CD spectra of **2d** with 3.0 equiv of 4,4′-dipyridyl in CH_2Cl_2. (c) An illustration depicting the orientational change of the porphyrins from "left-twisted" to "face-to-face" induced by 4,4′-dipyridyl.

coupling between the porphyrins attached to the β-sheet may reflect the left-twisted arrangement of the polypeptide strands [Fig. 7(c), left].

Fluorescence energy transfer between porphyrins bound to GS

The NMR, UV-vis and CD spectra described above strongly suggest that the orientation of porphyrins bound to GS differs in various solvents. We next examined the solvent effect on the fluorescence emission spectra, because (1) the emission of PorZn overlaps the absorption of PorFb, (2) PorFb and PorZn of **2dFbZn** are located in close proximity, (3) the energy transfer from the excited state PorZn to the ground state PorFb is expected to occur intramolecularly[5,6] and (4) the energy-transfer efficiency depends on the orientation of the porphyrins.[5] The fluorescence emission spectra of **2d** ($\lambda_{ex} = 516$ nm, $\lambda_{em} = 655$ and 719 nm, fluorescence quantum yield $\Phi_f = 0.10$) and **2dZn$_2$** ($\lambda_{ex} = 552$ nm, $\lambda_{em} = 608$ and 652 nm, $\Phi_f = 0.025$) in toluene are similar to those of FbTPP and ZnTPP, respectively.[32] These facts show that the two porphyrins in **2d** or **2dZn$_2$** are independent in the absorption and emission events.

Upon exciting **2dFbZn** in toluene at 552 nm, the emission appears at 608, 655 and 723 nm with intensities of 5.0, 70 and 24 (arbitrary units; trace A in Fig. 8, the fluorescence spectra in Fig. 8 are normalized for the absorption at λ_{ex}). PorFb absorbs 40% of the excitation incident light and PorZn 60% in **2dFbZn** [calculated from the ratio of ε_{552} of **2d** (28 600 M^{-1} cm^{-1}) and **2dZn$_2$** (42 200 M^{-1} cm^{-1})]. If no energy transfer occurs between the porphyrins of **2dFbZn** in the fluorescence event, the emission of **2dFbZn** should be equal to $0.40 \times$ **2d** $+ 0.60 \times$ **2dZn$_2$** (Fig. 8, trace B). However, the emission spectra of **2dFbZn** (Fig. 8, trace A) differed substantially from this calculated spectrum. Upon exciting **2dFbZn** in toluene at 516 nm, where PorFb absorbs 87% of the incident light, the emission is observed exclusively from PorFb (655 and 723 nm) and no emission from PorZn (608 nm, data not shown) is seem. These facts indicate that the excited state energy transfer occurs intramolecularly from the excited state of PorZn in **2dFbZn** to the ground state of PorFb.

From a comparison of the emission spectra of **2dFbZn** ($\lambda_{ex} =$ 552 nm; trace A in Fig. 8) and the calculated one assuming 0% energy transfer (trace B in Fig. 8), the emission of PorZn at 608 nm is 80% quenched, the emission of PorFb at 655 nm is 85% enhanced (after subtracting the residual emission from PorZn) and the emission of the PorFb at 723 nm is 99% enhanced. The decrease in the emission of PorZn corresponds to an increase in the emission of PorFb at 655 and 723 nm, supporting the mechanism of excited state energy transfer. The excitation spectrum of **2dFbZn**, monitoring the emission of PorFb ($\lambda_{em} = 723$ nm, data not shown), is different from the absorption spectra of **2dFbZn**, **2d** or **2dZn$_2$**. However, the excitation spectrum fits very well to the calculated spectra assuming 82% energy transfer, that is, the sum of the UV-vis spectra of **2d** $+ 0.82 \times$ **2dZn$_2$**. Thus, we assume the apparent energy-transfer efficiency of **2dFbZn** in toluene to be (at least) 82%.[5c] The other mechanisms for the quenching of the excited state of PorZn, such as excited state intersystem crossing to afford the triplet state and electron transfer from PorZn to PorFb, have been considered to be negligible.[5c] Of course, the exact energy-transfer efficiency should be obtained from the measurement of the excited state lifetime τ of PorZn. However, the lifetime of PorZn in **2dFbZn** seems to be below a nanosecond, because, for instance, the reported lifetime of ZnTPP is 2.0 ns (in toluene) and the lifetime of Zn porphyrin in phenylene–ethyne–phenylene linked dimers is as short as 24–90 ps.[5c] Because of the inaccessibility of ps-order time-resolved fluorescence or absorption spectroscopies, we used a semi-quantitative evaluation of the energy-transfer efficiency by steady-state fluorescence spectroscopy.

Steady-state fluorescence spectra were used to evaluate the energy-transfer efficiencies from PorZn to PorFb in **2dFbZn** not only in toluene as described above but also in MeOH, CH_2Cl_2 and DMF. Upon exciting the λ_{max} of PorZn at 549–557 nm of **2dFbZn**, three emissions appear at 603–609 nm (from PorZn), 653–655 nm (overlap of the emissions from the PorZn and PorFb) and 716–723 nm (from PorFb) in all the solvents examined. In all the solvents examined, the emission from PorZn at 603–609 nm decreases significantly compared with the calculated spectra assuming 0% energy transfer while the emission from PorFb is much larger than calculated. By averaging the quenching efficiency of the emission from PorZn at 603–609 nm and the enhancement of the emission of PorFb at 653–655 nm, the energy-transfer efficiencies in MeOH, CH_2Cl_2 and DMF were estimated to be 75, 65 and 60%, respectively. Trace C in Fig. 8 shows the emission spectra of **2dFbZn** in DMF, where the emission of PorZn at 609 nm decreases to 61%, the emission of PorFb at 654 nm is 58% enhanced (after subtracting the residual emission from the PorZn) and the emission of PorFb at 720 nm is 69% enhanced. Thus, the energy-transfer efficiency is in the order of toluene > MeOH > CH_2Cl_2 > DMF, which suggests that the distance between the PorZn and the PorFb is in the order of toluene < MeOH < CH_2Cl_2 < DMF. However, the possibility that the different energy-transfer efficiencies might be due to other solvent effects can not be neglected.

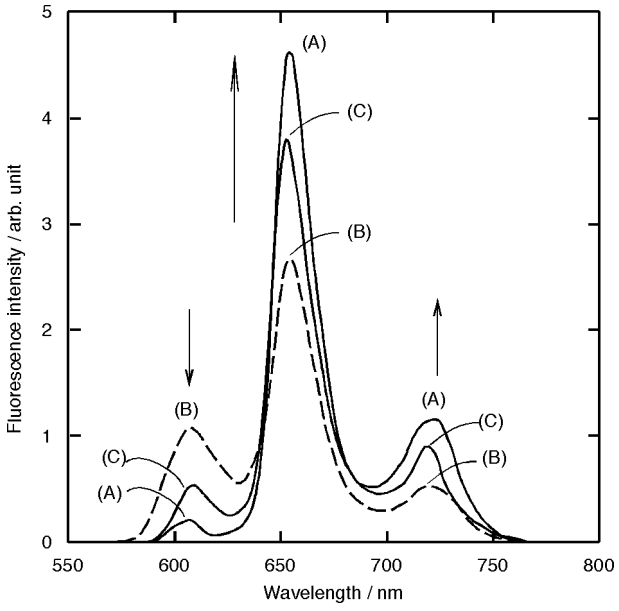

Fig. 8 Fluorescence emission spectra of **2dFbZn** ($\lambda_{ex} = 552$ nm) in toluene (trace A), a calculated spectrum assuming 0% energy transfer in toluene (trace B, broken line) and **2dFbZn** ($\lambda_{ex} = 557$ nm) in DMF (trace C).

Conclusion

The interaction between a pair of porphyrins bound to a natural cyclic peptide, Gramicidin S, was investigated by ^{1}H NMR, CD, UV-vis and fluorescence spectroscopy. ^{1}H NMR analyses indicate that two tolyl groups among the three tolyl groups of a porphyrin are high-field shifted by the ring current effect of the other porphyrin, which suggests a side-by-side arrangement of the porphyrins. The high-field shift and the signal line broadening are in the order toluene-d_8 > CD_2Cl_2 > DMF-d_7. The variable temperature NMR measurements in CD_2Cl_2 indicate a dynamic process involving the porphyrins. The high-field shifts of the ^{1}H NMR signals depend on the length of the spacer between the porphyrin and peptide, being in the order of **1d** < **3d** < **2d**. The exciton-coupled Cotton effects at the porphyrin Soret band region also characterize

the assorted structures of the porphyrins. The intensities are in the order: between two zinc porphyrins > between a zinc porphyrin and a free-base porphyrin ≈ between two free-base porphyrins. The Cotton effects are also solvent-dependent, with toluene > MeOH > triethyl phosphate > TFE > CH_2Cl_2 > pyridine > DMF, in which this order is in line with the solvent π* parameter. The efficiency of the intramolecular energy transfer from the excited state PorZn to the ground state PorFb are also solvent-dependent. The energy-transfer efficiencies are in the order of toluene > MeOH > CH_2Cl_2 > DMF, which is similar to the order observed in the ^{1}H NMR and CD spectra. In the solvents examined in this study, toluene is the most favorable solvent for the assembling of porphyrins. These findings hopefully will be utilized in a future study to build a more sophisticated porphyrin assembly on the polypeptide framework, and furthermore, possibly to control the structure and the function of the β-sheet polypeptide by conjugation with porphyrins.

Experimental

General

Amino acid derivatives were purchased from Watanabe Chemical (Hiroshima, Japan) and Wako Pure Chemical (Osaka, Japan), except for Boc–Orn(Fmoc)–OH from Bachem. ZnTMP (tetramesitylporphyrinato zinc) was synthesized as reported.[33]

HPLC was carried out with a Hitachi L-7100 pump and L-7420 UV-vis detectors (220 and 420 nm) using (1, normal phase) a Chemcosorb 100 Å silica gel column (4.6 × 150 mm, analytical, R_f^1) or a WakoSil-II 5Sil-100 silica gel column (10 × 250 mm, preparative) eluted with a linear gradient of 3–8% EtOH in toluene over 30 min with 1.0 (analytical) and 3.0 (preparative) mL min^{-1} flow rates and (2, analytical, reversed phase, R_f^2) a Wakopak C4 column (4.6 × 150 mm) eluted with a linear gradient of 68–95% CH_3CN–0.1% TFA over 10 min and then with 95% CH_3CN–0.1% TFA with a 1.0 mL min^{-1} flow rate.

^{1}H NMR spectra were measured on a JEOL JNM α-500 spectrometer (500 MHz), in which the chemical shifts were determined with respect to internal tetramethylsilane. T_1 was determined by the inversion recovery method with nonlinear curve fitting. FAB MS, including FAB HR-MS, were measured on a JEOL JMS-SX 102A mass spectrometer using 3-nitrobenzyl alcohol as a matrix unless otherwise noted. UV-vis (Hitachi U-2010) and CD (Jasco J-820) spectra were recorded using quartz cells of 1 and 10 mm path lengths at 298 K with 1.0 (UV) and 1.6 (CD) μM peptide concentration. The peptide concentrations were determined using $\varepsilon_{421} = 1\,070\,000$ M^{-1} cm^{-1} for **2d**, $\varepsilon_{421} = 772\,000$ M^{-1} cm^{-1} for **2dFbZn** and $\varepsilon_{424} = 795\,000$ M^{-1} cm^{-1} for **2dZn$_2$** in toluene, in which the concentration of the solutions were determined by amino acid analyses (Peptide Institute, Osaka, Japan). Fluorescence spectra were recorded on a Hitachi F-2500 fluorescence spectrophotometer equipped with a Hamamatsu R928F photomultiplier at 298 K, with a scan speed of 300 nm min^{-1}, 2.5 nm slit widths for both excitation and emission, a photomultiplier voltage of 400 V and a response of 0.04 s. In the measurement of the emission spectra, the absorptivity of the excitation wavelength was kept around 0.08, which means a *ca.* 1.5 μM peptide concentration. The fluorescence quantum yield Φ_f was obtained relative to the known values for FbTPP and TPPZn.[32]

Syntheses of the GS derivatives

See Electronic supplementary information (ESI).

Acknowledgements

We thank Professor Hideo Akisada and Ms. Junko Nishida at Kyushu Kyoritsu University for the CD measurements, Professor Masahiko Sisido at Okayama University for the fluorescence measurements, Dr. Masako Fujiwara at JEOL, Ltd., Japan, for the molecular modeling study, Ms. Keiko Yamaguchi at Kyushu Institute of Technology for the FAB MS measurements and also Dr. Yuji Tanaka and Mr. Takaaki Nakashima at Kyushu Institute of Technology for technical assistance. We also thank the referees for their constructive comments. This work was supported in part by Grants-in-aid for Scientific Research (Nos. 12650 869 and 15550 149) from the Ministry of Education, Culture, Sports, Science and Technology, Japan.

References

1 For a review, see: A. R. Battersby, *Nat. Prod. Rep.*, 2000, **17**, 507.
2 J. Deisenhofer, O. Epp, K. Miki, R. Huber and H. Michel, *Nature (London)*, 1985, **318**, 618; A. Zouni, H.-T. Witt, J. Kern, P. Fromme, N. Krauß, W. Saenger and P. Orth, *Nature (London)*, 2001, **409**, 739.
3 G. McDermott, S. M. Prince, A. A. Freer, A. M. Hawthornthwaite-Lawless, M. Z. Papiz, R. J. Cogdell and N. W. Isaacs, *Nature (London)*, 1995, **374**, 517; Y. Kobuke and K. Ogawa, *Bull. Chem. Soc. Jpn.*, 2003, **76**, 689.
4 S. Iwata, C. Ostermeier, B. Ludwig and H. Michel, *Nature (London)*, 1995, **376**, 660; T. Tsukihara, H. Aoyama, E. Yamashita, T. Tomizaki, H. Yamaguchi, K. Shinzawa-Itoh, R. Nakashima, R. Yaono and S. Yoshikawa, *Science*, 1995, **269**, 1069; N. Igarashi, H. Moriyama, T. Fujiwara, Y. Fukumori and N. Tanaka, *Nat. Struct. Biol.*, 1997, **4**, 276.
5 (*a*) R. L. Brookfield, H. Ellul, A. Harriman and G. Porter, *J. Chem. Soc., Faraday Trans. 2*, 1986, **82**, 219; (*b*) H. Tamiaki, K. Nomura and K. Maruyama, *Bull. Chem. Soc. Jpn.*, 1993, **66**, 3062; (*c*) J.-S. Hsiao, B. P. Krueger, R. W. Wagner, T. E. Johnson, J. K. Delaney, D. C. Mauzerall, G. R. Fleming, J. S. Lindsey, D. F. Bocian and R. J. Donohoe, *J. Am. Chem. Soc.*, 1996, **118**, 11181; (*d*) S. I. Yang, R. K. Lammi, J. Seth, J. A. Riggs, T. Arai, D. Kim, D. F. Bocian, D. Holten and J. S. Lindsey, *J. Phys. Chem. B*, 1998, **102**, 9426; (*e*) D. Holten, D. F. Bocian and J. S. Lindsey, *Acc. Chem. Res.*, 2002, **35**, 57; (*f*) N. Aratani, A. Osuka, H. S. Cho and D. Kim, *J. Photochem. Photobiol., C*, 2002, **3**, 25 and references cited therein.
6 N. Maruo, M. Uchiyama, T. Kato, T. Arai, H. Akisada and N. Nishino, *Chem. Commun.*, 1999, 2057; T. Kato, M. Uchiyama, N. Maruo, T. Arai and N. Nishino, *Chem. Lett.*, 2000, 144; T. Kato, N. Maruo, H. Akisada, T. Arai and N. Nishino, *Chem. Lett.*, 2000, 890; E. K. L. Yeow, K. P. Ghiggino, J. N. H. Reek, M. J. Crossley, A. W. Bosman, A. P. H. J. Schenning and E. W. Meijer, *J. Phys. Chem. B*, 2000, **104**, 2596; M. del Rosario Benites, T. E. Johnson, S. Weghorn, L. Yu, P. D. Rao, J. R. Diers, S. I. Yang, C. Kirmaier, D. F. Bocian, D. Holten and J. S. Lindsey, *J. Mater. Chem.*, 2002, **12**, 65; M.-S. Choi, T. Aida, T. Yamazaki and I. Yamazaki, *Chem.-Eur. J.*, 2002, **8**, 2668; K. Susumu and M. J. Therien, *J. Am. Chem. Soc.*, 2002, **124**, 8550; H. S. Cho, D. H. Jeong, S. Cho, D. Kim, Y. Matsuzaki, K. Tanaka, A. Tsuda and A. Osuka, *J. Am. Chem. Soc.*, 2002, **124**, 14 642 and references cited therein.
7 For reviews, see: J. K. M. Sanders, in *The Porphyrin Handbook*, eds. K. M. Kadish, K. M. Smith and R. Guilard, Academic Press, San Diego, 2000, vol. **3**, p. 347; J.-C. Chambron, V. Heitz and J.-P. Sauvage, in *The Porphyrin Handbook*, eds. K. M. Kadish, K. M. Smith and R. Guilard, Academic Press, San Diego, 2000, vol. **6**, p. 1; H. Ogoshi, T. Mizutani, T. Hayashi and Y. Kuroda, in *The Porphyrin Handbook*, eds. K. M. Kadish, K. M. Smith and R. Guilard, Academic Press, San Diego, 2000, vol. **6**, p. 279.
8 For reviews see: F. Nastri, A. Lombardi, L. D. D'Andrea, M. Sanseverino, O. Maglio and V. Pavone, *Biopolymers*, 1998, **47**, 5; A. Lombardi, F. Nastri and V. Pavone, *Chem. Rev.*, 2001, **101**, 3165.
9 C. T. Choma, K. Kaestle, K. S. Åkerfeldt, R. M. Kim, J. T. Groves and W. F. DeGrado, *Tetrahedron Lett.*, 1994, **35**, 6191; T. Arai, K. Kobata, H. Mihara, T. Fujimoto and N. Nishino, *Bull. Chem. Soc. Jpn.*, 1995, **68**, 1989; G. R. Geier III and T. Sasaki, *Tetrahedron*, 1999, **55**, 1859; T. Arai, A. Tsukuni, K. Kawazu, H. Aoi, T. Hamada and N. Nishino, *J. Chem. Soc., Perkin Trans. 2*,

2000, 1381; M. L. Kennedy, S. Silchenko, N. Houndonougbo, B. R. Gibney, P. L. Dutton, K. R. Rodgers and D. R. Benson, *J. Am. Chem. Soc.*, 2001, **123**, 4635; M. M. Rosenblatt, D. L. Huffman, X. Wang, H. A. Remmer and K. S. Suslick, *J. Am. Chem. Soc.*, 2002, **124**, 12394; Y. Takeuchi, H. Watanabe, A. Kashiwada, M. Nagata, T. Ohtsuka, N. Nishino, H. Kawai, T. Nagamura, Y. Kurono, N. Oku and M. Nango, *Chem. Lett.*, 2002, 848; K.-y. Tomizaki, H. Nishino, T. Arai, T. Kato and N. Nishino, *Chem. Lett.*, 2003, **32**, 6; T. Arai, M. Inudo, T. Ishimatsu, C. Akamatsu, Y. Tokusaki, T. Sasaki and N. Nishino, *J. Org. Chem.*, 2003, **68**, 5540 and references cited therein.

10 For instance, see: M. S. Searle, *J. Chem. Soc., Perkin Trans. 2*, 2001, 1011.

11 G. R. Moore, in *Protein Electron Transfer*, ed. D. S. Bendall, Bios Scientific, Oxford, 1996, p. 189.

12 C. A. Hunter, K. R. Lawson, J. Perkins and C. J. Urch, *J. Chem. Soc., Perkin Trans. 2*, 2001, 651; H.-J. Schneider, L. Tianjun, M. Sirish and V. Malinovski, *Tetrahedron*, 2002, **58**, 779 and the references cited therein.

13 Abbreviations used are according to the IUPAC-IUB commissions: *Eur. J. Biochem.*, 1984, **138**, 9. Other abbreviations: CD, circular dichroism; Dab, L-2,4-diaminobutyric acid (residue); GS, Gramicidin S; HR-MS, high-resolution mass spectroscopy; HOBt, 1-hydroxybenzotriazole; Orn, ornithine; oxime resin, *p*-nitrobenzophenone oxime resin; PorFb, 4-(10,15,20-tritolylporphyrin-5-yl)benzoyl or free-base porphyrin(s); PorZn, Zn complex of 4-(10,15,20-tritolylporphyrin-5-yl)benzoyl or Zn porphyrin(s); PyBOP, benzotriazol-1-yloxytripyrrolidinophosphonium hexafluorophosphate; TFA, trifluoroacetic acid; TFE, 2,2,2-trifluoroethanol; TPP, tetraphenylporphyrin;TMP, tetramesitylporphyrin.

14 For instance, see: (*a*) G. Némethy and H. A. Scheraga, *Biochem. Biophys. Res. Commun.*, 1984, **118**, 643; (*b*) N. Nishino, T. Arai, J. Hayashida, H. I. Ogawa, H. Yamamoto and S. Yoshikawa, *Chem. Lett.*, 1994, 2435; (*c*) T. Arai, T. Imachi, T. Kato, H. I. Ogawa, T. Fujimoto and N. Nishino, *Bull. Chem. Soc. Jpn.*, 1996, **69**, 1383; (*d*) D. Andreu, S. Ruiz, C. Carreno, J. Alsina, F. Albericio, M. Á. Jiménez, N. de la Figuera, R. Herranz, M. T. García-López and R. González-Muniz, *J. Am. Chem. Soc.*, 1997, **119**, 10579; (*e*) H. Mihara, J. Hayashida, H. Hasegawa, H. I. Ogawa, T. Fujimoto and N. Nishino, *J. Chem. Soc., Perkin Trans. 2*, 1997, 517; (*f*) E. J. Prenner, R. N. A. H. Lewis and R. N. McElhaney, *Biochim. Biophis. Acta*, 1999, **201**, 1462 and the references cited therein.

15 (*a*) T. Arai, N. Maruo, Y. Sumida, C. Korosue and N. Nishino, *Chem. Commun.*, 1999, 1503; (*b*) T. Arai, K. Araki, K. Fukuma, T. Nakashima, T. Kato and N. Nishino, *Chem. Lett.*, 2002, 1110.

16 G. Ösapay and J. W. Taylor, *J. Am. Chem. Soc.*, 1992, **114**, 6966; G. Ösapay and M. Goodman, *J. Chem. Soc., Chem. Commun.*, 1993, 1599; W. Zhang and J. W. Taylor, *Tetrahedron Lett.*, 1996, **37**, 2173; N. Nishino, J. Hayashida, T. Arai, H. Mihara, Y. Ueno and H. Kumagai, *J. Chem. Soc., Perkin Trans. 1*, 1996, 939 and references cited therein.

17 M. Waki, O. Abe, R. Okawa, T. Kato, S. Makisumi and N. Izumiya, *Bull. Chem. Soc. Jpn.*, 1967, **40**, 2904.

18 E. M. Krauss and S. I. Chan, *J. Am. Chem. Soc.*, 1982, **104**, 6953; M. Tamaki, S. Akabori and I. Muramatsu, *Bull. Chem. Soc. Jpn.*, 1993, **66**, 3113.

19 Y. Kiso, K. Ukawa and T. Akita, *J. Chem. Soc., Chem. Commun.*, 1980, 101; H. Yajima, Y. Minamitake, S. Funakoshi, Y. Hirai and T. Nakajima, *Chem. Pharm. Bull.*, 1981, **29**, 1752.

20 T. Higashijima, T. Miyazawa, M. Kawai and U. Nagai, *Biopolymers*, 1986, **25**, 2295; A. C. Bach II, C. J. Eyermann, J. D. Gross, M. J. Bower, R. L. Harlow, P. C. Weber and W. F. DeGrado, *J. Am. Chem. Soc.*, 1994, **116**, 3207 and references cited therein.

21 A. Pardi, M. Billeter and K. Wüthrich, *J. Mol. Biol.*, 1984, **180**, 741G. W. Vuister, M. Tessari, Y. Karimi-Nejad and B. Whitehead, in *Biological Magnetic Resonance*, Modern Techniques in Protein NMR series, vol. **16**, eds. N. R. Krishna and L. J. Berliner, Kluwer, New York, 1999, p. 195.

22 G. Wagner, D. Neuhaus, E. Wörgötter, M. Vasák, J. H. R. Kägi and K. Wüthrich, *J. Mol. Biol.*, 1986, **187**, 131.

23 (*a*) J. Sandström, *Dynamic NMR Spectroscopy*, Academic, London, 1982; (*b*) C. L. Perrin and T. J. Dwyer, *Chem. Rev.*, 1990, **90**, 935; (*c*) R. L. Jarek, R. J. Flesher and S. K. Shin, *J. Chem. Educ.*, 1997, **74**, 978.

24 (*a*) M. J. Crossley, L. G. Mackay and A. C. Try, *J. Chem. Soc., Chem. Commun.*, 1995, 1925; (*b*) T. Arai, K. Takei, N. Nishino and T. Fujimoto, *Chem. Commun.*, 1996, 2133; (*c*) N. Berova and K. Nakanishi, in *Circular Dichroism: Principles and Applications*, eds. N. Berova, K. Nakanishi and R. W. Woody, John Wiley and Sons, New York, 2nd edn., 2000, p. 337; (*d*) T. Sagawa, S. Fukugawa, T. Yamada and H. Ihara, *Langmuir*, 2002, **18**, 7223; (*e*) T. Hayashi, T. Aya, M. Nonoguchi, T. Mizutani, Y. Hisaeda, S. Kitagawa and H. Ogoshi, *Tetrahedron*, 2002, **58**, 2803; (*f*) V. V. Borovkov, T. Harada, Y. Inoue and R. Kuroda, *Angew. Chem., Int. Ed.*, 2002, **41**, 1378; (*g*) G. Pescitelli, S. Gabriel, Y. Wang, J. Fleischhauer, R. W. Woody and N. Berova, *J. Am. Chem. Soc.*, 2003, **125**, 7613 and references cited therein.

25 M.-C. Hsu and R. W. Woody, *J. Am. Chem. Soc.*, 1971, **93**, 3515.

26 C. Reichardt, *Solvents and Solvent Effects in Organic Chemistry*, VCH, Weinheim, 2nd edn., 1988.

27 (*a*) O. W. Kolling, *J. Am. Chem. Soc.*, 1979, **18**, 1175; (*b*) M. J. Kamlet, J.-L. M. Abboud, M. H. Abraham and R. W. Taft, *J. Org. Chem.*, 1983, **48**, 2877; (*c*) C. Laurence, P. Nicolet, M. T. Dalati, J.-L. M. Abboud and R. Notario, *J. Phys. Chem.*, 1994, **98**, 5807.

28 M. Kasha, H. R. Rawls and M. A. El-Bayoumi, *Pure Appl. Chem.*, 1965, **11**, 371.

29 P. Hambright, in *The Porphyrin Handbook*, eds. K. M. Kadish, K. M. Smith and R. Guilard, Academic Press, San Diego, 2000, vol. **3**, p. 129 and references cited therein.

30 I. P Danks, T. G. Lane, I. O. Sutherland and M. Yap, *Tetrahedron*, 1992, **48**, 7679.

31 M. J. E. Steinberg and J. M. Thornton, *Nature (London)*, 1978, **271**, 15; W. F. DeGrado, C. M. Summa, V. Pavone, F. Nastri and A. Lombardi, *Annu. Rev. Biochem.*, 1999, **68**, 779.

32 P. G. Seybold and M. Gouterman, *J. Mol. Spectrosc.*, 1969, **31**, 1.

33 J. S. Lindsey and R. W. Wagner, *J. Org. Chem.*, 1989, **54**, 828.